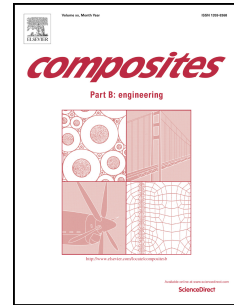


Journal Pre-proof

Synthesis of an organophosphorus flame retardant derived from daidzein and its application in epoxy resin

Chao Ma, Juan Li



PII: S1359-8368(19)32152-3

DOI: <https://doi.org/10.1016/j.compositesb.2019.107471>

Reference: JCOMB 107471

To appear in: *Composites Part B*

Received Date: 14 May 2019

Revised Date: 20 September 2019

Accepted Date: 20 September 2019

Please cite this article as: Ma C, Li J, Synthesis of an organophosphorus flame retardant derived from daidzein and its application in epoxy resin, *Composites Part B* (2019), doi: <https://doi.org/10.1016/j.compositesb.2019.107471>.

This is a PDF file of an article that has undergone enhancements after acceptance, such as the addition of a cover page and metadata, and formatting for readability, but it is not yet the definitive version of record. This version will undergo additional copyediting, typesetting and review before it is published in its final form, but we are providing this version to give early visibility of the article. Please note that, during the production process, errors may be discovered which could affect the content, and all legal disclaimers that apply to the journal pertain.

© 2019 Published by Elsevier Ltd.

Synthesis of an organophosphorus flame retardant derived from daidzein and its application in epoxy resin

Chao Ma^{1,2}, Juan Li^{1,2}

1. Ningbo Key Laboratory of Polymer Materials, Ningbo Institute of Materials Technology and Engineering, Chinese Academy of Sciences, Ningbo, 315201, China.
2. Center of Materials Science and Optoelectronics Engineering, University of Chinese Academy of Sciences, Beijing, 100049, China.

ABSTRACT

For the concern of sustainable and green chemical engineering, the development of flame retardants from renewable biomaterials is particularly attractive. Daidzein is an isoflavone found in large amounts in soybeans and other legumes. The structure of daidzein permits easy reaction with flame retardant groups and is beneficial for the formation of char at high temperature. A flame retardant which can work in both the gas phase and the condensed phase may be unusually effective. An organophosphorus flame retardant (DPOD) has been prepared using daidzein and diphenylphosphinyl chloride, and used to modify the flammability of epoxy (EP) resin. The structure and flame retardant mode of action of DPOD in EP were explored. The results showed that DPOD works in both the gas phase and the condensed phase and improves the flame retardancy of EP blends greatly. In addition, the DPOD doesn't deteriorate the glass transition temperature and impact strength of EP blends. This work is a useful attempt to use biobased monomers in the design of flame retardants.

Keywords Daidzein; Epoxy; Flame retardancy; Gas phase; Condensed phase

1. Introduction

Epoxy (EP) resin is an important thermosetting material and has been widely used in electrical laminates, binders and coatings due to its excellent performance [1,2]. However, the flammability of EP brings some security risks when used in electrical and electronic sectors, aerospace industries, public transport, etc. For most applications, it is necessary to improve the flame retardancy of EP. Traditionally, many halogen compounds have been used as flame retardants for EP. Though they have excellent flame-retardant performance, they may release some corrosive, toxic gases and smoke during combustion, which is harmful to human health and natural ecosystem [3]. More importantly, these compounds readily migrate from polymer matrix into environment. They may tend to bioaccumulation and pose threats to human health [4]. They have been detected in environment, wildlife and human body [5]. Because of its wide distribution in the environment and negative influence on human health, developing green flame retardants [6], such as phosphorus [7, 8], nitrogen [9], silicon [10], layered double hydroxides (LDH) [11, 12] and ferrocene [13] compounds are gaining increasing attention.

Among these, phosphorus flame retardants occupy an important position because of their good flame retardant efficiency and low toxicity. Phosphorus flame retardants with appropriate structure may work in both gas and condensed phase [14-16] and may play an efficient flame retardant role in polymers which is expected to be the result. Here, appropriate structure is the key to playing a dual role. Recently, it has been shown that diphenyl phosphine oxide (DPO) derivatives can act in the gas phase to improve the flame retardancy of polymers [17, 18]. Two kinds of co-curing agents, DOPO-PHE and DPO-PHE (**Scheme S1**) for EP have been synthesized using 9,10-dihydro-9-oxygen-10-phosphorus heterophenanthrene-10-oxide (DOPO) and

DPO [19], respectively. With the same phosphorus content, DPO-PHE not only showed better flame retardant performance than DOPO-PHE in EP, but also exhibited better characteristics such as little impact on glass transition temperature (T_g), thermal stability and water absorption of EP. This suggests that DPO with a right structure may act as better flame retardant than DOPO in EP. Therefore, the utilization of DPO derivatives may be a good strategy for modification of the flammability of EP.

An appropriate structure is the key factor for a flame retardant. DPO can react with compounds containing amino or hydroxyl groups, thus many derivative structures can be obtained. To obtain a DPO derivative which work in both the gas phase and condensed phase, the selected structure should have good char formation ability at high temperature. Compared with compounds from petrochemical sources, compounds from renewable biomaterials are particularly attractive [20]. Some biobased compounds, including those from lignin [21], isosorbide [22], gallic acid [23], phloroglucinol [24], vanillin [25, 26], cardanol [27] have been employed as flame retardants. Daidzein is an isoflavone found in large amounts in soybeans and other legumes. An intrinsically flame-retardant EP [28] has been prepared by using daidzein. Due to the good char layer formed during combustion, the EP could achieve the UL-94 V-0 rating. This indicated that the daidzein is a good component to form char. Therefore, when DPO and daidzein are combined into a molecule, the product may have the advantages of both. Thus an efficient flame retardant with both gas phase and condensed phase effects for EP may be obtained. This has not been reported previously.

In this work, the aim is to synthesis a flame retardant by using daidzein and diphenylphosphinyl chloride which may work in both the gas phase (effect of DPO) and the condensed phase (effect of daidzein).. The obtained DPO-daidzein compound

(DPOD) will be used to modify the flammability of EP. The flame retardancy, flame retardant mode of action, thermo degradation behaviors and mechanical properties of EP/DPOD blends are studied comprehensively.

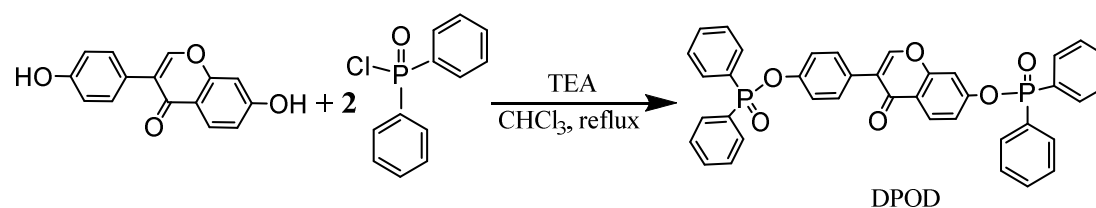
2. Experimental section

2.1 Materials

Daidzein, diphenylphosphinyl chloride and 4,4'-diaminodiphenylmethane (DDM) were procured from Energy Chemical Company (Shanghai, China). Triethylamine, trichloromethane and ethanol were acquired from Sinopharm Chemical Reagent Co. Ltd (Shanghai, China). Sodium bicarbonate was purchased from Aladdin Industrial Co., Ltd (Shanghai, China). Diglycidyl ether of bisphenol A (DGEBA, E-44) was supplied by Yangzi Petrochemical Co. Ltd (Nanjing, China). All materials were used without further purification.

2.2 Synthesis of DPOD

Daidzein (12.7 g, 0.05 mol), triethylamine (10.1 g, 0.100 mol), $MgCl_2$ (0.05 g) and 500 mL $CHCl_3$ were added into a 1000 mL, three-neck glass flask equipped with a mechanical stirrer, reflux condenser and thermometer. Diphenylphosphinyl chloride (23.7 g, 0.100 mol) in 30 ml $CHCl_3$ was added dropwise at room temperature over 20 min. The mixture was heated to reflux temperature and kept for 8h. Then, the mixture was distilled to remove $CHCl_3$ and the DPOD was obtained. The product was washed by saturated sodium bicarbonate solution and ethanol for three times, respectively, and then vacuum-dried at 80 °C for 24h (yield, 95%). The reaction route of DPOD is shown in **Scheme 1**.



Scheme 1. Synthetic route of DPOD.**2.3 Preparation of flame retardant EP blends**

DPOD was added into DGEBA with continuous stirring at 80 °C until they were mixed well. After that, the solution was mixed with DDM. And the mixture was degassed for 5 min at reduced pressure, poured rapidly into a preheated PTFE mold and then cured at 120 °C for 2 h and 170 °C for another 4 h. Then the sample was cooled down to room temperature. The formulation of EP/ DPOD is listed in **Table 1**.

Table 1 Formulation of EP blends

Samples	DGEBA [*] (wt%)	DDM [*] (wt%)	DPOD (wt%)	P content (wt%)
EP	82.1	17.9	0	0
EP/DPOD4	78.8	17.2	4	0.38
EP/DPOD6	77.1	16.9	6	0.56
EP/DPOD8	75.5	16.5	8	0.75

^{*} During curing process, the amount of EP and active amine (-NH-) is equal.

2.4 Characterization

NMR analyses were performed by using a 400 AVANCE spectrometer (Bruker, Germany) at room temperature. CDCl₃ was used as solvent for ¹³C NMR, and DMSO-d₆ was used for ¹H NMR and ³¹P NMR.

UL-94 vertical burning test was conducted using a 5400 vertical burning tester (SuzhouYangYi Vouch Testing Technology Co., Ltd., China) with sample dimensions of 100 mm × 13 mm × 3.2 mm according to ASTM D3801.

Limiting oxygen index (LOI) test was performed using a 5801 digital oxygen index analyzer (SuzhouYangYi Vouch Testing Technology Co., Ltd, China) with bar

dimensions of 100 mm × 6.5 mm × 3.2 mm according to ASTM D2863-97.

A FTT Cone Calorimeter (Fire Testing Technology, UK) was used to study the heat release behaviors of EP blends with a heat flux of 35 kW·m⁻² according to ISO 5660. The sample dimension is 100 mm × 100 mm × 3 mm.

Thermal gravimetric analysis (TGA) was performed using a TGA/DSC Analyzer (Mettler Toledo, Switzerland). About 4 mg samples were heated from 50 °C to 800 °C in a nitrogen or air atmosphere (50 mL/min) at a heating rate of 10 °C/min.

FTIR tests were recorded using a 6700 FT-IR spectrometer (Nicolet, USA) at 4 cm⁻¹ revolution from 400~4000 cm⁻¹. KBr pellets were used.

Thermal gravimetric analysis linked with infrared spectra (TG-FTIR) was conducted on either a TGA/DSC1 analyzer (Mettler Toledo, Switzerland) interfaced to a Nicolet 6700 FTIR spectrometer (Thermo fisher, USA) (for EP/DPOD blends) or a TGA 8000 analyzer (PerkinElmer, USA) interfaced to a Spectrum Two FTIR spectrometer (PerkinElmer, USA) (for DPOD). And the temperature of transfer line between TG and FTIR was 200 °C and 270 °C. About 10 mg EP/DPOD blends or 4 mg DPOD were heated from 50 °C to 800 °C in a nitrogen atmosphere (50 mL/min) at a heating rate of 10 °C/min. The spectra were collected every 40 s for 80 min.

The morphology of char residues for EP and EP/DPOD blends after the UL-94 test were investigated using an EVO18 (Zeiss, Germany) scanning electron microscope (SEM).

The phosphorus content in char residue was measured by an inductively coupled plasma optical emission spectrometry method (ICP-OES) using a PerkinElmer Optima 2100DV apparatus (PerkinElmer, USA). Sample preparation for ICP-OES

referred to the previous literature [29].

The pyrolysis behaviors of samples were tested using a pyrolysis-gas chromatography /mass spectroscopy (Py-GC/MS) in helium atmosphere. The samples (300 μg) were heated from ambient to 600 $^{\circ}\text{C}$ and kept for 20 s in a pyrolyzer (Frontier Lab PY-3030D, Japan). Then, the volatile products were separated by gas chromatography (Shimadzu GC-2010 Plus, Japan) and analyzed by mass spectroscopy (Shimadzu MS-QP 2010SE, Japan). The column temperature was held at 40 $^{\circ}\text{C}$ for 3 min and increased to 300 $^{\circ}\text{C}$ at a rate of 15 $^{\circ}\text{C}/\text{min}$ and kept for 10 min. The temperature of EI source was set as 230 $^{\circ}\text{C}$, and the temperature of transfer line was kept at 260 $^{\circ}\text{C}$.

A Triple TOF 4600 Q-TOF mass spectrometer (AB Sciex, USA) was used to test the products of DPOD after thermal treatments. The Q-TOF mass spectrometer was run in an atmospheric pressure chemical ionization (APCI) interface using a positive ion mode. The ion spray voltage was 5500 V. The declustering potential was 80 V. The temperature of vaporizer was 300 $^{\circ}\text{C}$. The injection rate was 5 $\mu\text{L}/\text{min}$. The mass range for the MS investigation was set as $m/z = 50 - 2000$.

Dynamic mechanical analysis (DMA) tests were carried using a TA Q800 Instrument (TA, USA) in a tension fixture mode. All the samples with the dimension of 20 mm \times 6.5 mm \times 0.5 mm were tested from 25 to 250 $^{\circ}\text{C}$ at a heating rate of 3 $^{\circ}\text{C}/\text{min}$ and a frequency of 1 Hz.

A GT-7045-HMH impact tester (Gotech Testing Machines CO. LTD., China) was used to test the notched impact strength of EP blends according to ISO179-1:98 with the use of 1 J pendulum.

3. Results and discussion

3.1 Synthesis and characterization of DPOD

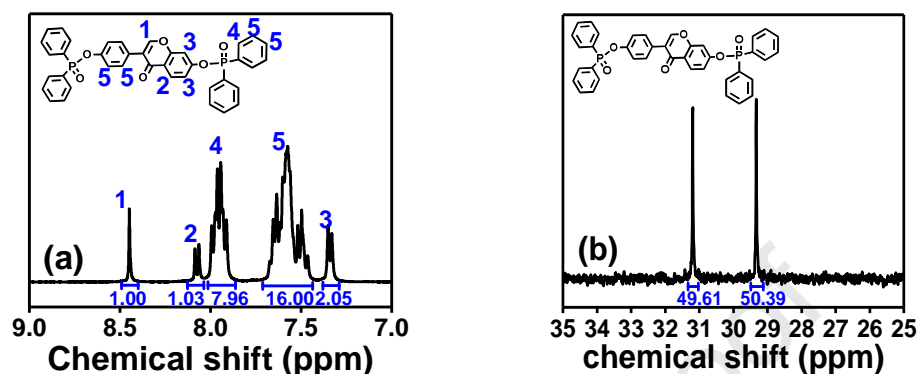


Fig. 1. (a) ^1H NMR and (b) ^{31}P NMR spectra of DPOD.

DPOD was synthesized by using diphenylphosphinyl chloride and daidzein. The chemical structure of DPOD was characterized by NMR and FTIR. **Fig. 1(a)** shows the local enlargement in ^1H NMR spectrum of DPOD and the assignment of hydrogen atoms. The whole ^1H NMR spectrum is shown in **Fig. S1**. The peak at 8.45 ppm is attributed to the hydrogen atom 1 in oxygen-containing heterocycle. The peaks at 8.06 ppm and 8.08 ppm belong to the hydrogen atom 2 of fused heterocycle. The peaks at 7.33 ppm and 7.34 ppm correspond to the hydrogen atoms 3, which are close to the $-\text{OP}(\text{O})\text{Ph}_2$ group in space. The peaks at 7.84-8.00 ppm belong to the hydrogen atoms 4 near phosphorus atom, and the peaks at 7.32-7.71 ppm are attributed to the hydrogen atoms 5 away from phosphorus atoms. Moreover, the ratio of area that belongs to these two sets of peaks is 7.96:16 which is close to 8:16. Therefore it coincides with the number ratio of corresponding hydrogen atoms in DPOD meaning that the target product has been successfully prepared.

The ^{31}P NMR spectrum of DPOD is presented in **Fig. 1(b)**. There are two peaks

at 29.3 and 31.2 ppm, corresponding to the phosphorus atom in OP(O)Ph₂ group. Because of incompletely symmetric structure of daidzein, the phosphorus atoms have slightly different chemical shift. For peaks belong to phosphorus atoms, the ratio of areas is 49.6: 50.4 (approximately 1: 1), which suggests DPOD has a complete structure. In addition, the ¹³C NMR spectrum of DPOD is showed in **Fig. S2**, and all peaks match well with the carbon atoms of DPOD. In addition, the FTIR spectra of daidzein, diphenylphosphinyl chloride and DPOD are showed in **Fig. S3**. The results further prove the structure of DPOD. Both the NMR and FTIR results suggest that DPOD is obtained successfully.

3.2 Thermal degradation behaviors of DPOD

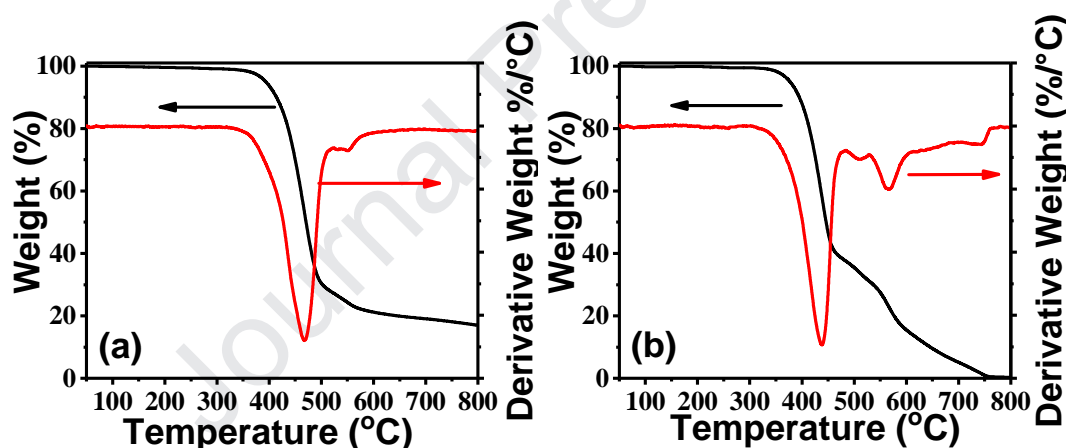


Fig. 2. TGA and DTG curves of DPOD in (a) nitrogen and (b) air.

Fig. 2 shows the TGA and DTG curves of DPOD in nitrogen and air atmosphere. $T_{5wt\%}$ refers to the temperature at 5% weight loss. The TGA curve of DPOD in nitrogen shows two thermal degradation stages, correspondingly, there are two peaks in the DTG curve. The first degradation stage is from 393 °C to 502 °C accompanied by a weight loss of 70%. The second stage is small and ranges from 502 °C to 600 °C. The $T_{5wt\%}$ of DPOD is 393 °C, indicating that thermal stability of DPOD is good

enough for the processing of most polymers. Besides, there is 17 wt% char residue at 800 °C, which may provide some condensed phase effect during combustion.

Fig. 2(b) shows the thermal degradation behavior of DPOD in air, which is more complex than that in nitrogen. The TGA curve of DPOD in air shows no less than three thermal degradation stages. The main decomposition stage is from 377 °C to 485 °C with a weight loss of 60.0% which is attributed to the decomposition of diphenyl phosphine oxide and daidzein. Then there are two thermal degradation stages from 485 °C to 762 °C indicates the further thermal-oxide decomposition of the unstable char layer. The $T_{5wt\%}$ of DPOD in air is 377 °C due to oxidation in air, which is 16 °C lower than that in nitrogen. Besides, there are few char residues at 800 °C.

3.3 Flame retardancy of EP/DPOD blends

LOI and UL-94 vertical burning tests are two common methods to evaluate the flame retardancy of polymers. The corresponding data of EP blends from the two tests are listed in **Table 2**. Neat EP is easy to be ignited and is not be classified (NC) in the UL-94 test. Adding 4 wt% DPOD into EP, the LOI of EP/DPOD4 is increased to 33.3%, and obtains the UL-94 V-1. When 6 wt% DPOD is added into EP, the burning time (t_1/t_2) of EP/DPOD6 is reduced significantly. The EP/DPOD6 achieves the UL-94 V-0 rating without dripping and has a LOI value of 34.7%. With the content of DPOD increasing, the flame retardant performance enhance further. The results suggest that the DPOD is an efficient flame retardant for EP.

Table 2 UL-94 rating and LOI value of EP/DPOD blends

Samples	LOI (%)	UL-94 (3.2mm)		
		t_1/t_2 (s) ^a	Dripping	Ignition Rating

EP	25.0	>60/-	Y	Y	NC
EP/DPOD4	33.3	26.03/5.58	N	N	V-1
EP/DPOD6	34.7	4.98/2.96	N	N	V-0
EP/DPOD8	35.3	4.14/3.04	N	N	V-0

^a Represents the burning time after the first and second 10 s flame application.

3.4 TGA of EP/DPOD blends

The TGA and DTG of EP blends in nitrogen are exhibited in **Fig. 3** and the data are summarized in **Table 3**. The maximum weight loss rate is defined as V_{max} , and the temperature at V_{max} is defined as T_{max} . The char yield is marked as CY . The $CY_{800-cal}$ is calculated according to the weight percentage of EP and DPOD in blends, and the $CY_{800-exp}$ refers to the experimental value at 800 °C.

All EP blends present similar single decomposition stage like neat EP in nitrogen atmosphere, but their TGA curves shift to lower temperature than that of EP. For example, the $T_{5wt\%}$ for EP/DPOD6 is 351 °C which is 19°C lower than neat EP. This suggests that DPOD promotes the thermal degradation of EP resin. In addition, the V_{max} for all EP/DPOD blends are smaller than EP indicating that DPOD slows the degradation of EP at higher temperature.

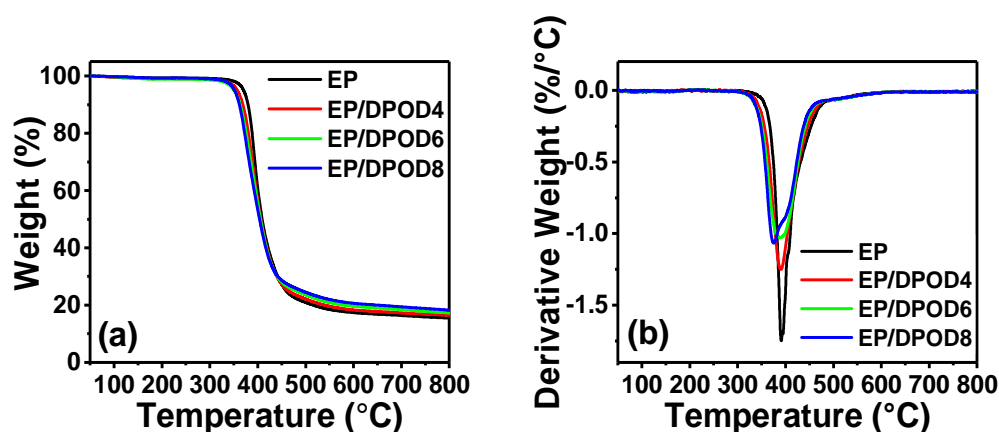


Fig. 3. (a)TGA and (b) DTG curves of EP blends in nitrogen atmosphere.

Table 3 TGA data of EP blends in nitrogen atmosphere.

Samples	$T_{5wt\%}$ (°C)	T_{max} (°C)	V_{max} (%/°C)	$CY_{800-cal}$ (%)	$CY_{800-exp}$ (%)
EP	370	391	1.74	-	15.5
EP/DPOD4	356	391	1.25	15.5	16.5
EP/DPOD6	350	389	1.02	15.6	17.3
EP/DPOD8	351	376	1.06	15.6	18.3

The TGA and DTG curves of EP blends in air are exhibited in **Fig. 4** and the detailed data are summarized in **Table 4**. In air atmosphere, all samples show two-stage decomposition and all TGA curves of EP/DPOD blends shift to lower temperature slightly. The first stage takes place between 352 °C and 470 °C, and the second is from 470 °C to 668 °C. The $T_{5wt\%}$ and T_{max} of EP blends shift to lower temperature compared to pure EP, which is similar to the results in nitrogen atmosphere. In addition, the char formed in air is not stable enough, so these char intermediates continue to decompose above 500 °C, resulting in few char residues at 800 °C. The first V_{max} for all EP/DPOD blends are smaller with EP suggesting that DPOD slows the degradation of EP. However the second V_{max} for EP/DPOD blends change slightly compared to EP. This means the char formed in air is not stable, and will decompose at high temperature.

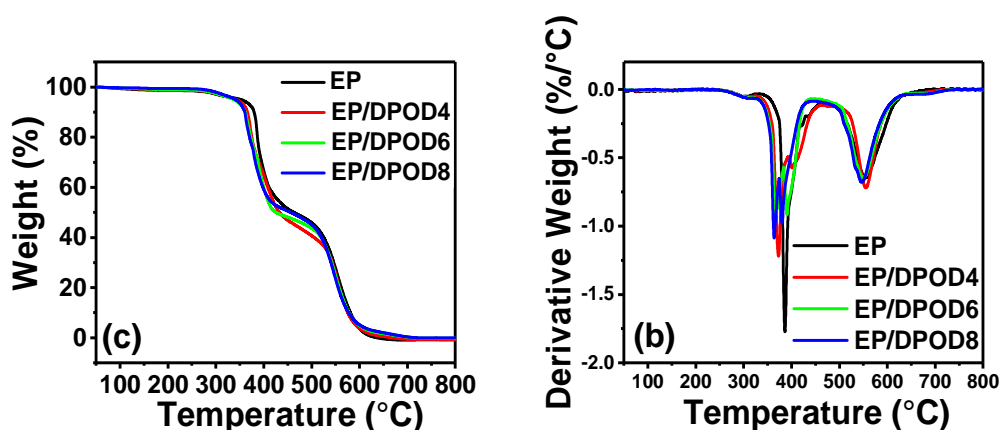
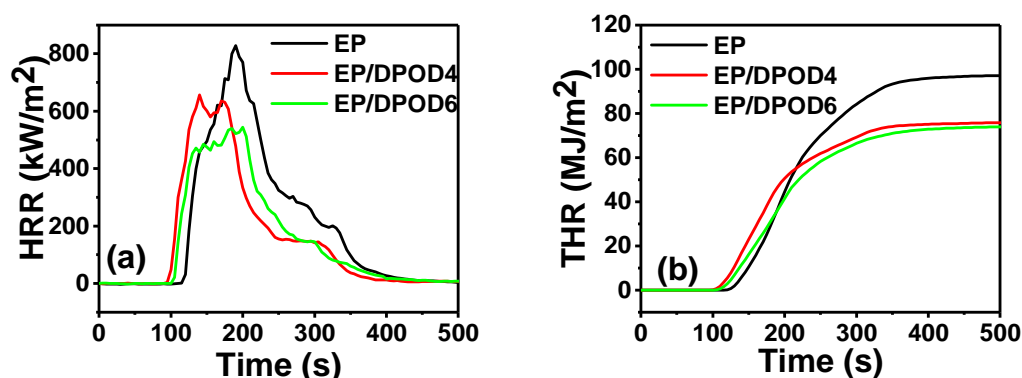


Fig. 4. (a) TGA and (b) DTG curves of EP blends in air atmosphere.**Table 4** TGA data of EP blends in air atmosphere.

Samples	$T_{5\%}$ (°C)	T_{max} (°C)		V_{max} (%/°C)	
		1 st	2 nd	1 st	2 nd
EP	352	386	556	1.77	0.65
EP/DPOD4	342	373	554	1.22	0.71
EP/DPOD6	337	366	550	0.92	0.64
EP/DPOD8	341	363	547	1.07	0.68

3.5 Cone calorimetry results of EP/DPOD blends

Cone calorimetry (CC) is an important way to evaluate the combustion characteristics of polymer materials. The time to ignition (TTI), peak of heat release rate (pHRR), time to pHRR (t_{pHRR}), effective heat of combustion (EHC), total heat released (THR), and the char residue yield are listed in **Table 5**. **Fig. 5** shows the relationships between HRR, THR, smoke production release (SPR), CO₂ release rate, CO release rate, mass and time.



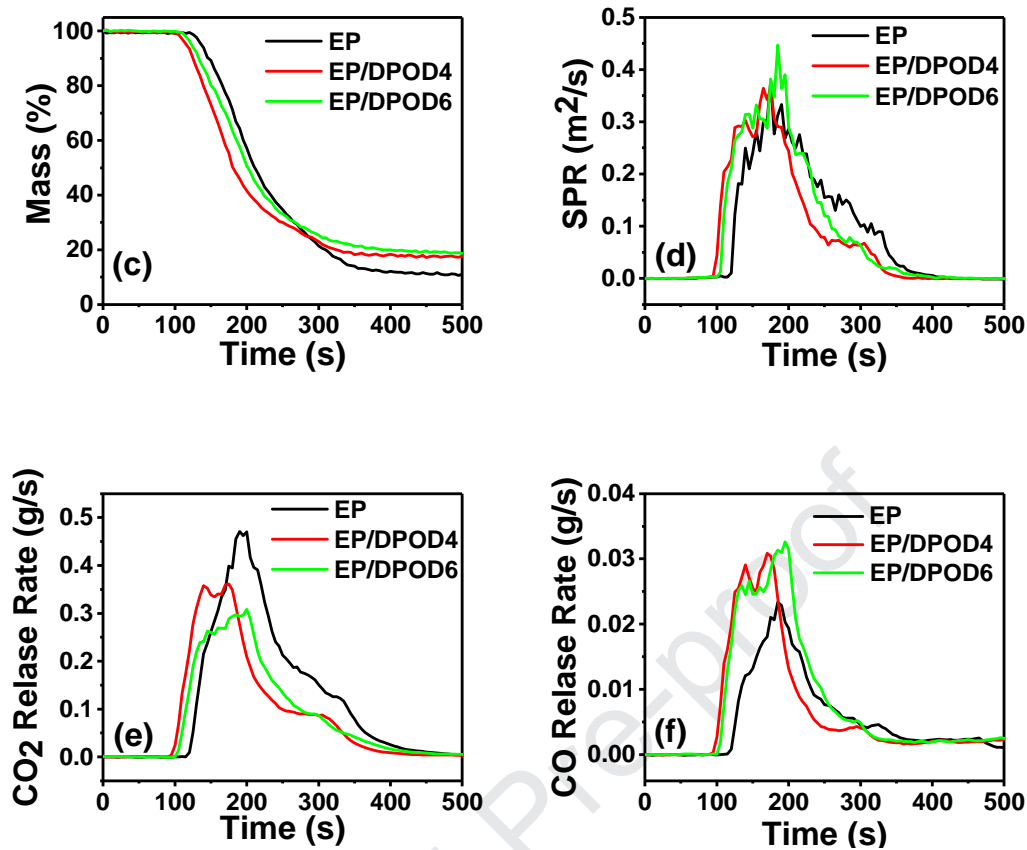


Fig. 5. Relationships between (a) HRR, (b) THR, (c) mass, (d) SPR, (e) CO₂ release rate, (f) CO release rate and time for EP blends.

Table 5 Cone calorimetry data of EP blends

Samples	TTI (s)	pHRR (kW/m ²)	t_{pHRR} (s)	EHC (MJ/kg)	THR (MJ/m ²)	Residue (%)
EP	118	827	200	22.5	97.2	10.5
EP/DPOD4	97	657	140	20.6	75.8	17.5
EP/DPOD6	103	544	200	18.3	74.8	18.2

The pHRR of EP is 827 kW/m². Adding 4wt% DPOD into EP, the pHRR is decreased to 657 kW/m². Increasing the content of DPOD to 6wt%, the pHRR of EP/DPOD6 is 544 kW/m², which is 34% lower than EP. The THR is decreased to 74.8

MJ/m² from 97.2 MJ/m² for EP. The average EHC is also reduced from 22.5 MJ/kg for EP to 18.3 MJ/kg for EP/DPOD6. The reductions of pHRR, THR and EHC are consistent with flame retardant effect of DPOD in gas phase [19], which is attributed to the PO radicals produced by DPOD. The TTI reflects the ignitability of EP blends, which is 118 s for EP. For EP/DPOD4 and EP/DPOD6, the TTI is shortened to 97 s and 103 s, meaning that they are ignited earlier than EP. This may attribute to the chemical reactions between DPOD and EP at high temperature. Moreover, the TTI of EP/DPOD6 is slightly longer than EP/DPOD4. As previous report [30,31], when the concentration of fuel from material degradation reaches a critical value, ignition happens. The longer ignition time means less fuel decomposed from EP/DPOD6, which benefits from great radical quench effect of DPOD in vapor phase. **Fig. 5(c)** presents the mass curves of EP blends. Compared with EP, the EP/DPOD shows an apparent increase in char residue, which is similar to TGA. It illustrates that EP/DPOD could produce more char layer during burning, which can protect inner resin from flame. SPR of EP blends changes slightly means the DPOD has few smoke suppression effects. In addition, **Fig. 5(e)** and **(f)** show the CO₂ and CO release rate of EP blends. Compared with neat EP, the CO₂ release rate of EP/DPOD is decreased, but the CO release rate is increased slightly. The PO radicals degraded by DPOD may scavenge the H and OH radicals in the flame, leading an incomplete combustion. Moreover, partly oxidized intermediates of EP blends increase SPR [32]. Besides, the decrease of OH radicals weaken the conversion from CO to CO₂ [33], thus the CO release rate of EP/DPOD is higher than that of neat EP. These results suggest that DPOD works in gas phase mainly.

3.5 Morphology of char for EP blends

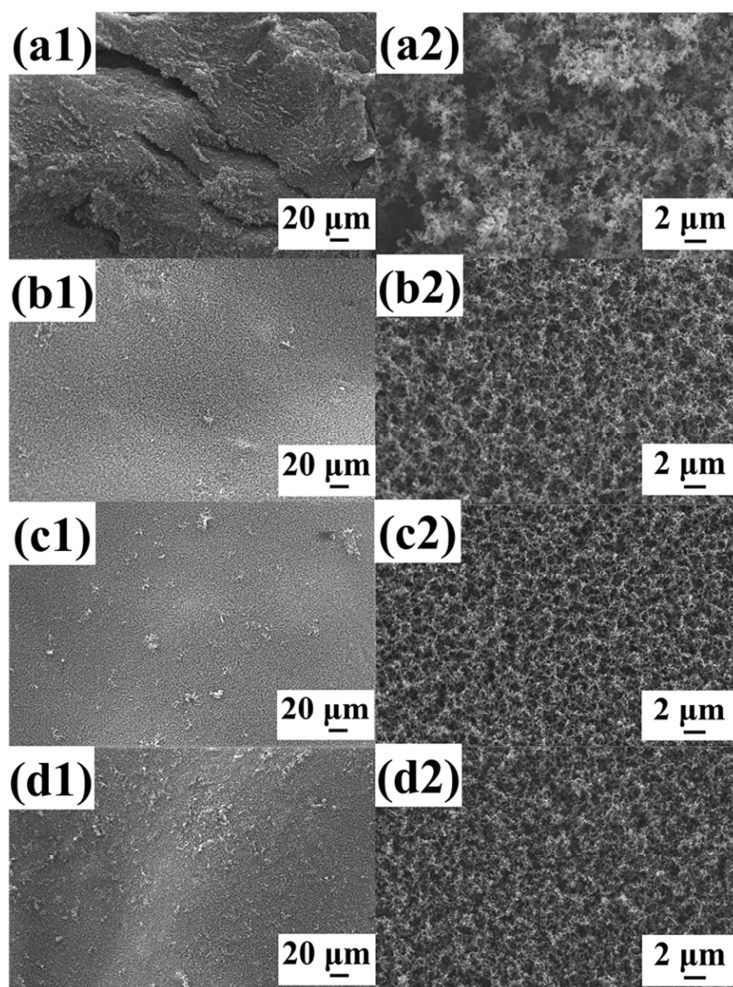


Fig. 6. SEM micrographs of char for (a1, a2) EP, (b1, b2) EP/DPOD4, (c1, c2) EP/DPOD6 and (d1, d2) EP/DPOD8.

Apart from char quantity, the morphology of char is another critical factor for EP blends to achieve good flame retardancy. **Fig. 6** displays the SEM micrographs of char after UL-94 tests for different EP blends. There are some obvious cracks and holes in char of EP. This char layer could not prevent the transmission of heat, oxygen and combustible gases, thus can't protect the internal resin from flame. When DPOD is added into EP, the char layers become dense and continuous, which acts as a good barrier for EP resin. Besides, there are some char particles covered on the surface of the char layer in EP/DPOD blends. This should be some small char particles suspended in the air during burning, when their size increases to a certain extent they

will be deposited on the surface of the char layer. Magnifying the char layer, some micropores are observed for both EP and EP/DPOD blends. For EP, the size of micropores ranges from a few microns to a dozen microns. While for EP/DPOD blends, the size of micropore is less than 1 micron. The smaller the size, the more difficult it is for gas and heat to diffuse. Thus, a better barrier effect is obtained.

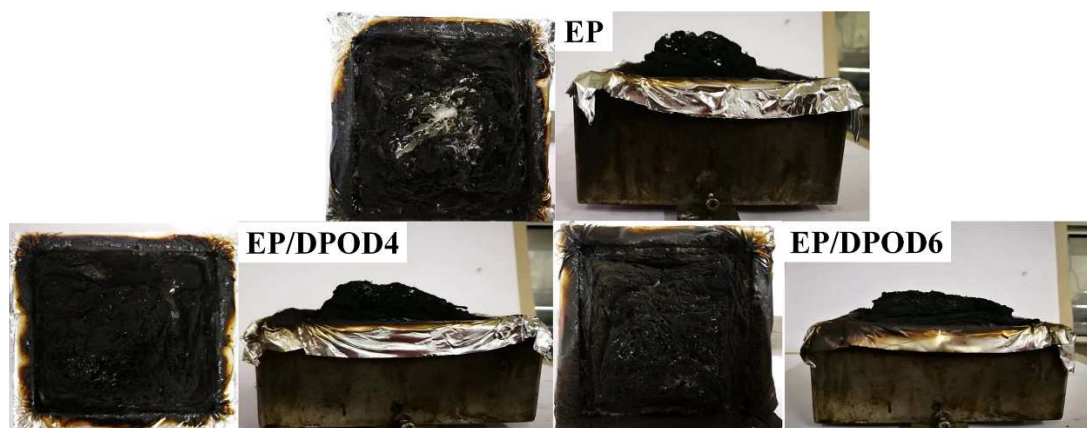


Fig. 7. Digital photos of EP blends after cone calorimetry tests.

The digital photos of EP blends after cone calorimetry tests are shown in **Fig. 7.** and **Fig. S4.** The EP forms a small amount of char, so there are large flaws in the middle of the char layer. When the DPOD was added into EP, the char amount is enhanced evidently and the char is more complete. The amount of defects decreases for the char layer of EP/DPOD4 and EP/DPOD6. A perfect char layer plays an important role in preventing heat, oxygen and combustible gas exchange and improving the flame retardancy of EP blends. Therefore, this is another reason for the improved flame retardancy of EP blends.

3.6 Flame retardant mode of action of DPOD in EP

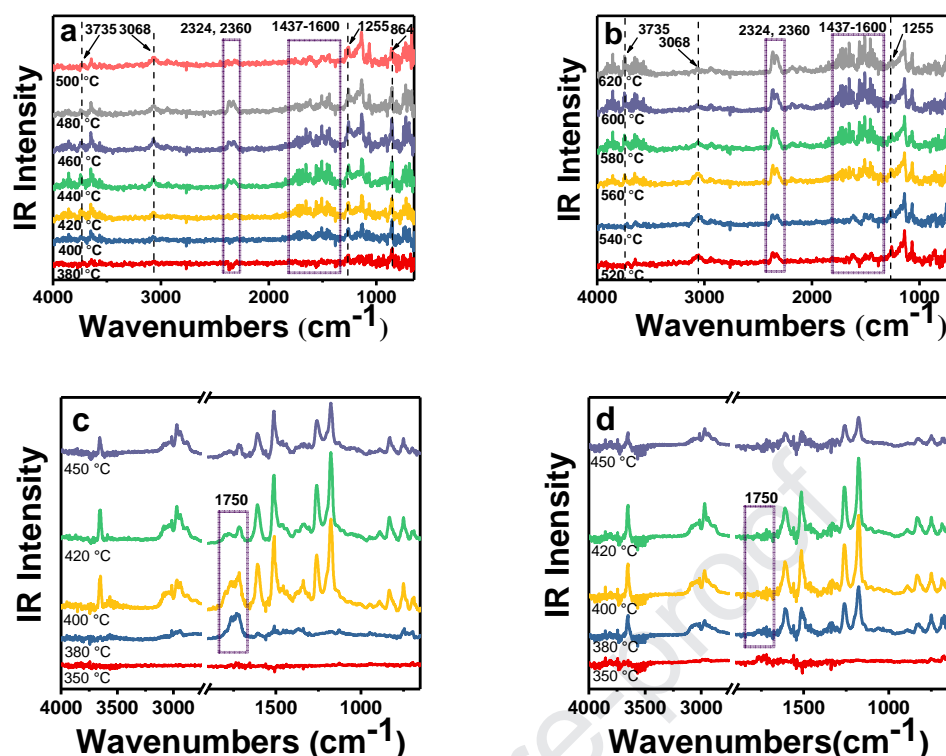


Fig. 8. TG-FTIR of gaseous products for (a, b) DPOD, (c) EP and (d) EP/DPOD6

TG-FTIR was used to analyze the gaseous products of DPOD, EP and EP blends during thermal degradation. The results are shown in **Fig. 8**. For DPOD, the assignment of the absorption peaks are presented in **Table S1** and the main pyrolysis products are phenol derivatives (3735 cm^{-1}), CO_2 (2324 cm^{-1} and 2360 cm^{-1}), phosphorus - containing compounds (1255 cm^{-1}) and aromatic compounds (1437 cm^{-1} to 1600 cm^{-1}). There are few FTIR peaks before $380\text{ }^\circ\text{C}$ for DPOD. When the temperature is increased to $400\text{ }^\circ\text{C}$, the peaks from 1437 cm^{-1} to 1600 cm^{-1} (aromatic compounds) appear and peak intensity at 1255 cm^{-1} (P=O) significantly increases, which is attributed to the decomposition of DPO. This is consistent with the first degradation stage of DPOD in TGA, and these phosphorus-containing products can exert a quenching effect in the gas phase during combustion of EP [34]. When the temperature is higher than $500\text{ }^\circ\text{C}$, the peak intensity of P=O becomes weak. Most phosphorus elements have entered into gas phase. After the temperature rises to

560 °C, the peak intensity of aromatic compounds increases again. This is caused by the degradation of unstable char [35].

As shown in **Fig. 8(c)**, the main degradation products of EP are phenol derivatives/H₂O (3650 cm⁻¹), CO₂ (2307-2380 cm⁻¹), ethers (1260 cm⁻¹), aromatic compounds (3010-3030, 1510, 825, 748 cm⁻¹) and hydrocarbons (2800-3100 cm⁻¹ and 1100-1250 cm⁻¹) [36,37]. As for EP/DPOD6, it can be seen that peak of carbonyl compound (1750 cm⁻¹) vanished, while no other significantly difference in degradation products. This means DPOD changes the thermal degradation process of EP. It is possible that new absorbance bands from DPOD, such as 1255 cm⁻¹ (P=O), coincide with that of degradation products of EP resin [38].

The char residues of EP and EP/DPOD6 after UL-94 tests were analyzed to research the effect of DPOD in condensed phase. The results are shown in **Fig. 9**. Comparing with EP, two additional peaks at 1433 cm⁻¹ (P-Ph) and 1130 cm⁻¹ (P-O-C) appear in the FTIR spectra of EP/DPOD. However, the intensity of the two peaks is low, so the phosphorus content in the condensed phase should be low. To further investigate the distribution of P in gas and condensed phase, the char was tested by ICP-OES and the results are shown in **Table 6**. Unsurprisingly, about 89 wt% P enter the gas phase during the burning process, and there is about 11 wt% P remained in the condensed phase. During combustion, the P in condensed phase will be degraded into H₃PO₃, H₃PO₄, or H₄P₂O₇ etc. and help EP to form char [5], which is important for protecting the underlying resin from burning.

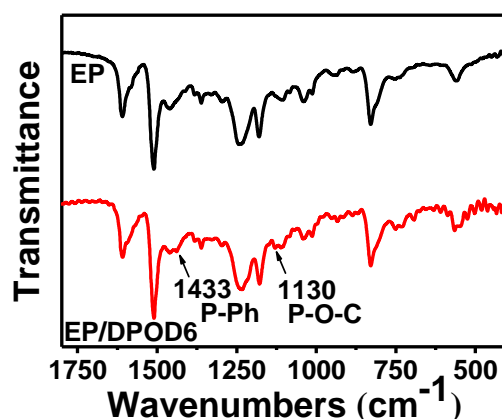


Fig. 9. FTIR spectra of char residues after UL-94 test

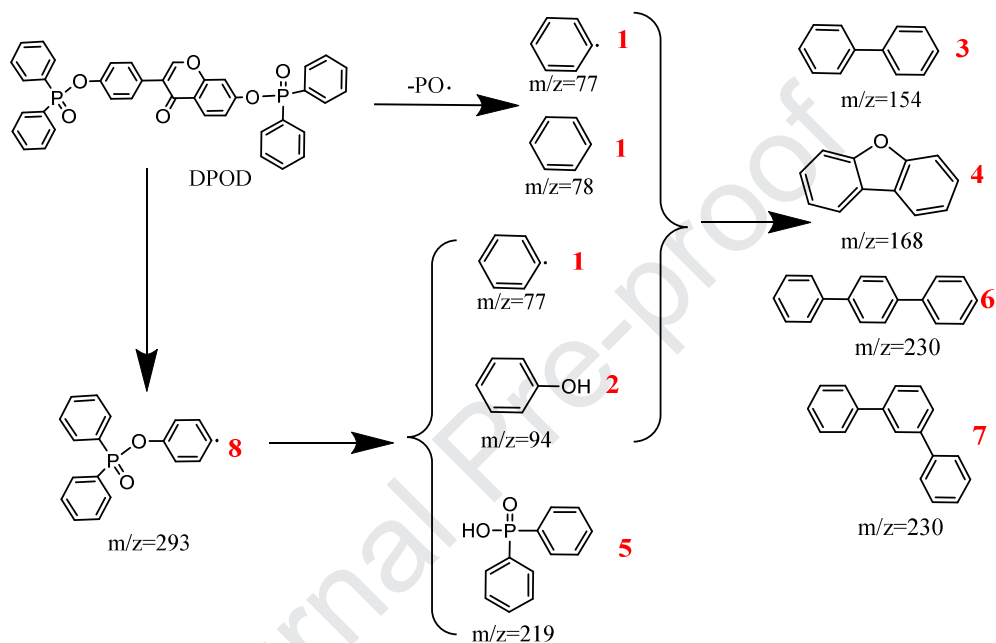
Table 6 ICP data of EP/DPOD6

Sample	P in EP/DPOD6 (wt%)	P in char ^a (wt%)	Char yield (wt%)	P in condensed phase ^b (wt%)
EP/DPOD6	0.56	0.42	15	11

^a Phosphorus content of char measured by ICP-OES. ^b Retention rate of phosphorus in condensed phase before and after combustion.

The reactions in EP/DPOD blends are complicated, to simplify the process, the pyrolysis behavior of single DPOD was tested by using Py-GC/MS. The total ion chromatogram and chemical structures of pyrolysis products are shown in **Fig. S5** and **Table S2**, the possible pyrolysis route of DPOD is illustrated in **Scheme 2**. The P-C bond firstly cleavages and produces benzene ($m/z=78$, peak 1) and benzene radical ($m/z=77$, peak 1), accompanied by the generation of PO radical with the temperature increasing. The peak of $m/z=78$ is strongest in total ion chromatogram, which means the cleavage of P-C bond is a main degradation reaction. Besides, the C-C bond of daidzein structure may fracture, producing phenyl diphenylphosphinate radical ($m/z=293$, peak 8), and further be decomposed into benzene radical ($m/z=77$, peak 1), phenol ($m/z=94$, peak 8) and diphenylphosphinic acid ($m/z=219$, peak 5). It is worth

pointing out there are no products from benzopyrone structure of DPOD in the Py-GC/MS. So the benzopyrone may participate in the cross-linking reactions and become char in the condensed phase. In summary, the PO radical can trap H and HO radicals in vapor phase and combine the terminal radical of EP chains, then inhibit some decomposition reactions.



Scheme 2. Possible pyrolysis route of DPOD

In order to understand the degradation process of DPOD further, a thermal decomposition experiment was attempted. The DPOD was placed in a glass tube and heated on an alcohol lamp for 10 s, 20 s and 30 s, respectively. After that, the residues were dissolved in DMSO and measured by Q-TOF mass spectrometer, and the results are shown in **Fig. 10** and **Table S3**. The Q-TOF mass spectra show that the products of DPOD after thermal treatment include diphenylphosphonic acid (compound I), daidzein (compound II), daidzein monophosphonate (compound III). When heating, the DPOD is degraded into compound III and compound I, then compound III is

further degraded into compound II and compound I (**Scheme 3**). With the extension of heating time, the intensity of compounds II, III decreases evidently, which suggests further degradation reactions take place and the char is formed meanwhile.

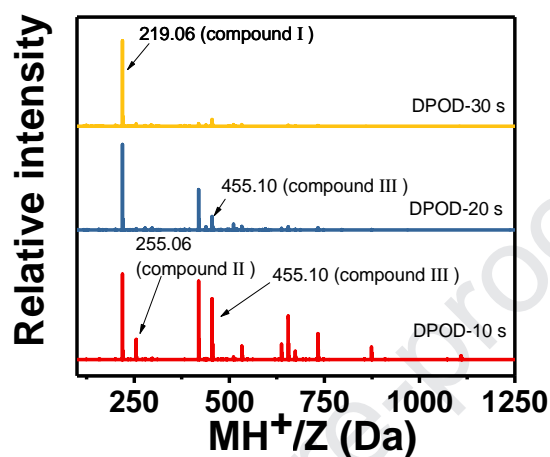
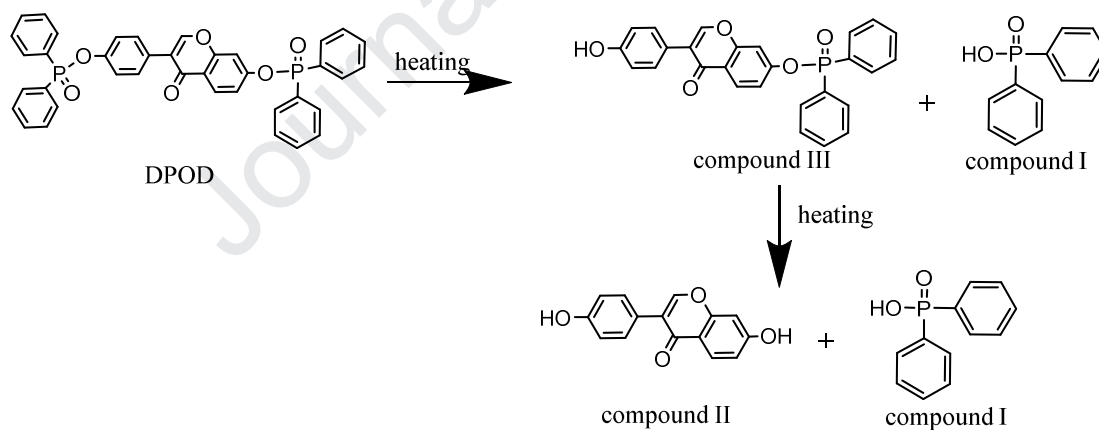
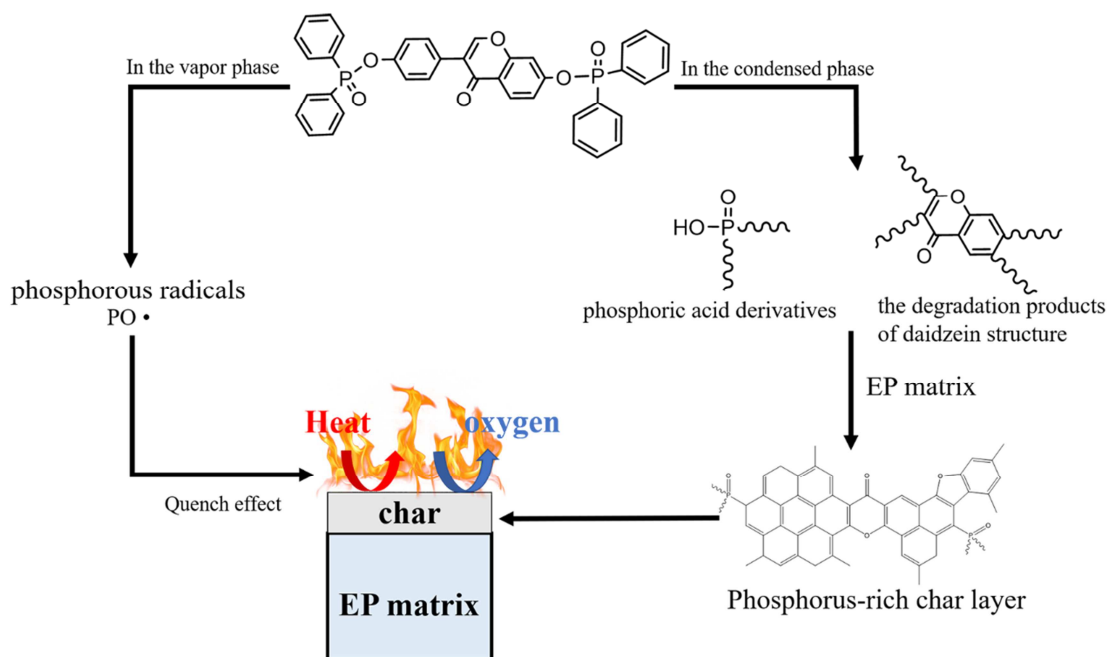


Fig. 10. Q-TOF mass spectra of DPOD after heating for different time



Scheme 3. Thermal degradation route of DPOD based on Q-TOF mass spectra



Scheme 4. Flame retardant mode of action of DPOD in EP

Combining with above results, the flame retardant mode of action of DPOD in EP is illustrated in **Scheme 4**. DPOD acts in both vapor and condensed phase, and the former is the main one during combustion. In the vapor phase, DPOD degrades and produces phosphorous radicals (PO radicals), which quench H, O and OH radicals produced by EP chain. In the condensed phase, DPOD produces phosphoric acid derivatives (such as diphenylphosphonic acid) and degradation products of daidzein. Because of its P-OH structure, the phosphoric acid derivatives react with these degradation products of daidzein and EP during thermal degradation, leading to a phosphorus-rich char layer. At the same time, a large amount of overflow gas leads to foaming of char layer. The DPOD regulates the formation of char and the generation of gases, thus reduces the defects of char and induces the formation of uniform microporous char. It is the comprehensive effects of these factors resulting in good flame retardancy.

3.7 Dynamic mechanical analysis and impact properties of EP blends

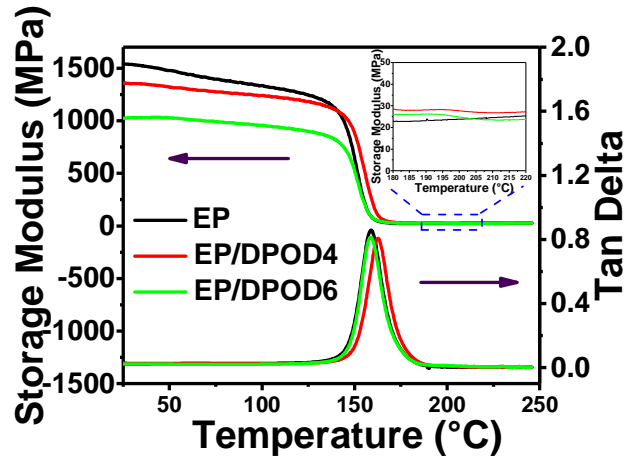


Fig. 11. Relationships between E' , $\tan \delta$ and temperature for EP and EP/DPOD blends.

Table 7 DMA data and impact strength of EP blends

Samples	T_g (°C)	E' (MPa)		$\nu_e (\times 10^3)$ mol/m ³	Impact strength (MPa)
		Glassy region ^a	Rubbery region ^b		
EP	159	1534	23.7	3.4	4.30 ± 0.81
EP/DPOD4	163	1353	27.3	4.0	5.12 ± 0.90
EP/DPOD6	159	1029	24.9	3.6	4.15 ± 0.33

^a E' at 30 °C. ^b E' at ($T_g + 40$) °C.

Fig. 11 presents the relationships between storage modulus (E'), tan delta ($\tan \delta$) and temperature for EP and EP/DPOD blends. The peak of $\tan \delta$ is defined as T_g . E' value reflects the stiffness of material. With the incorporation of DPOD, the E' at 30 °C for EP blends decreases evidently, while the T_g changes slightly. This means that DPOD reduces the rigidity of EP, which is due to the plasticization of DPOD and the mobility of EP molecular chains at low temperature is improved. **Table 7** lists the T_g and calculation results of cross-link density (ν_e) of EP and EP/DPOD, the ν_e was calculated based on the theory of rubber elasticity and the calculation equation is as

follow [28]

$$v_c = E'/3RT \quad (1)$$

where E' is the storage modulus of the cured resins in the rubbery region ($T_g + 40$ °C), T is the absolute temperature, and R is the gas constant. With the addition of DPOD, the v_c and T_g of EP blends are improved slightly compared to that of the EP. Although the increment is small, it will not deteriorate the performance of the EP at least. Besides, the impact strength of EP and EP/DPOD was tested and the results are listed in **Table 7**. The impact strength of EP/DPOD4 is 19% higher than EP, while that for the EP/DPOD6 is almost the same as that of EP. In summary, DPOD does improve the flame retardancy of EP without reducing its T_g and impact strength. This is helpful to develop flame retardant EP blends.

4. Conclusions

An organophosphorus flame retardant (DPOD) derived from daidzein and DPO was synthesized. The DPOD plays a good flame retardant role in EP resin. The EP blends with 6 wt% DPOD achieve the UL-94 V-0 rating, and a LOI value of 34.7%. The pHRR of EP/DPOD6 is also decreased evidently in cone calorimetry test. Moreover, DPOD does not deteriorate the glass transition temperature and impact strength of EP blends suggest. The flame retardant mode of action of DPOD in EP is summarized as follows. On the one hand, the DPOD produces PO radicals in the gaseous phase for quenching effect, some combustion reactions are terminated. On the other hand, DPOD produces phosphoric acid derivatives which react with degradation products of daidzein and EP to form char layer. Meanwhile, the gas flow

from decomposition leads to foaming of char layer. The DPOD regulates the formation of char and gas, thus reducing the defects of char, and induces the formation of uniform microporous char, which plays a good barrier role. It is the dual effects of DPOD in both the gas phase and the condensed phase improve the flame retardancy of EP. This is a useful exploration to design flame retardants derived from renewable biomaterials for EP.

Acknowledgements

This work is supported financially by the National Natural Science Foundation of China (Nos. 51973229, 51473178) and the Program for Ningbo Innovative Research Team (No. 2015B11005).

References

- [1] Liu S, Chevali VS, Xu Z, Hui D, Wang H. A review of extending performance of epoxy resins using carbon nanomaterials. *Compos B Eng* 2018;136:197-214.
- [2] Jin FL, Li X, Park SJ. Synthesis and application of epoxy resins: A review. *J Ind Eng Chem*. 2015;29:1-11.
- [3] Zhang M, Buekens A, Li X. Brominated flame retardants and the formation of dioxins and furans in fires and combustion. *J Hazard Mater* 2016;304:26-39.
- [4] Howell BA, Sun W. Biobased flame retardants from tartaric acid and derivatives. *Polym Degrad Stabil* 2018;157:199-211.
- [5] Yu G, Bu Q, Cao Z, Du X, Xia J, Wu M, et al. Brominated flame retardants (BFRs): A review on environmental contamination in China. *Chemosphere* 2016;150:479-90.
- [6] Papaspyrides CD, Kiliaris P. *Polymer Green Flame Retardants*. Newnes, 2014.

- [7] Liu L, Xu Y, Xu M, Li Z, Hu Y, Li B. Economical and facile synthesis of a highly efficient flame retardant for simultaneous improvement of fire retardancy, smoke suppression and moisture resistance of epoxy resins. *Compos B Eng* 2019;167:422-33.
- [8] Zhao XM, Yang LW, Martin FH, Zhang XQ, Wang R, Wang DY. Influence of phenylphosphonate based flame retardant on epoxy/glass fiber reinforced composites (GRE): Flammability, mechanical and thermal stability properties. *Compos B Eng* 2017;110:511-9.
- [9] Rao WH, Hu ZY, Xu HX, Xu YJ, Qi M, Liao W, et al. Flame-retardant flexible polyurethane foams with highly efficient melamine salt. *Ind Eng Chem Res* 2017;56(25):7112-9.
- [10] Liu C, Chen T, Yuan C, Chang Y, Chen G, Zeng B, et al. Highly transparent and flame-retardant epoxy composites based on a hybrid multi-element containing POSS derivative. *RSC Adv* 2017;7(73):46139-47.
- [11] Kalali EN, Wang X, Wang DY. Functionalized layered double hydroxide-based epoxy nanocomposites with improved flame retardancy and mechanical properties. *J Mate Chem A* 2015;3(13):6819-26.
- [12] Li Z, Liu ZQ, Dufosse F, Yan LK, Wang DY. Interfacial engineering of layered double hydroxide toward epoxy resin with improved fire safety and mechanical property. *Compos B Eng* 2018;152:336-46.
- [13] Liao DJ, Xu QK, McCabe RW, Babu HV, Hu XP, Pan N, et al. Ferrocene-based nonphosphorus copolymer: synthesis, high-charring mechanism, and its application in fire retardant epoxy resin. *Ind Eng Chem Res* 2017;56(44):12630-43.
- [14] Salmeia KA, Gaan S. An overview of some recent advances in DOPO-derivatives: Chemistry and flame retardant applications. *Polym Degrad Stabil*

2015;113:119-34.

[15] Wang P, Cai ZS. Highly efficient flame-retardant epoxy resin with a novel DOPO-based triazole compound: thermal stability, flame retardancy and mechanism. *Polym Degrad Stabil* 2017;137:138-50.

[16] Qian L, Qiu Y, Wang J, Xi W. High-performance flame retardancy by char-cage hindering and free radical quenching effects in epoxy thermosets. *Polymer*. 2015;68(Supplement C):262-9.

[17] Zhang H, Xu M, Li B. Synthesis of a novel phosphorus-containing curing agent and its effects on the flame retardancy, thermal degradation and moisture resistance of epoxy resins. *Polym Adv Technol* 2016;27(7):860-71.

[18] Wei YX, Deng C, Zhao ZY, Wang YZ. A novel organic-inorganic hybrid SiO₂@DPP for the fire retardance of polycarbonate. *Polym Degrad Stabil* 2018;154:177-85.

[19] Zhao J, Dong X, Huang S, Tian X, Song L, Yu Q, et al. Performance comparison of flame retardant epoxy resins modified by DPO-PHE and DOPO-PHE. *Polym Degrad Stabil* 2018;156:89-99.

[20] Costes L, Laoutid F, Brohez S, Dubois P. Bio-based flame retardants: When nature meets fire protection. *Mater Sci Eng R-Rep* 2017;117:1-25.

[21] Alalykin AA, Vesnin RL, Kozulin DA. Preparation of modified hydrolysis lignin and its use for filling epoxy polymers and enhancing their flame resistance. *Russ J Appl Chem* 2011;84(9):1616.

[22] Daniel YG, Howell BA. Flame retardant properties of isosorbide bis-phosphorus esters. *Polym Degrad Stabil* 2017;140:25-31.

[23] Howell BA, Oberdorfer KL, Ostrander EA. Phosphorus flame retardants for polymeric materials from gallic acid and other naturally occurring

- multihydroxybenzoic acids. *Int J Polym Sci* 2018;7237236.
- [24] Toldy A, Tóth N, Anna P, Marosi G. Synthesis of phosphorus-based flame retardant systems and their use in an epoxy resin. *Polym Degrad Stabil* 2006; 91(3):585-92.
- [25] Gu LQ, Chen GA, Yao YW. Two novel phosphorus-nitrogen-containing halogen-free flame retardants of high performance for epoxy resin. *Polym Degrad Stabil* 2014;108:68-75.
- [26] Lin CH, Chou YC, Shiao WF, Wang MW. High temperature, flame-retardant, and transparent epoxy thermosets prepared from an acetovanillone-based hydroxyl poly(ether sulfone) and commercial epoxy resins. *Polymer* 2016;97:300-8.
- [27] Wang X, Zhou S, Guo WW, Wang PL, Xing WY, Song L, et al. Renewable cardanol-based phosphate as a flame retardant toughening agent for epoxy resins. *ACS Sustain Chem Eng* 2017;5(4):3409-16.
- [28] Dai JY, Peng YY, Teng N, Liu Y, Liu CC, Shen XB, et al. High-performing and fire-resistant biobased epoxy resin from renewable sources. *ACS Sustain Chem Eng* 2018;6(6):7589-99.
- [29] Liu C, Yao Q. Design and Synthesis of Efficient Phosphorus Flame Retardant for Polycarbonate. *Ind Eng Chem Res* 2017;56(31):8789-96.
- [30] Jing J, Zhang Y, Tang XL, Fang ZP. Synthesis of a highly efficient phosphorus-containing flame retardant utilizing plant-derived diphenolic acids and its application in polylactic acid. *RSC Adv* 2016;6(54):49019-27.
- [31] Zhao XM, Guerrero FR, Lorca J, Wang DY. New superefficiently flame-retardant bioplastic poly(lactic acid): flammability, thermal decomposition behavior, and tensile properties. *ACS Sustain Chem Eng* 2016;4(1):202-9.
- [32] König A, Kroke E. Flame retardancy working mechanism of methyl-DOPO and

- MPPP in flexible polyurethane foam. *Fire Mater* 2012;36(1):1-15.
- [33] Bastin B, Paleja R, Lefebvre J. Fire behavior of polyurethane foams. *J Cell Plast* 2003;39(4):323-40.
- [34] Yang S, Wang J, Huo SQ, Wang M, Cheng LF. Synthesis of a phosphorus/nitrogen-containing additive with multifunctional groups and its flame-retardant effect in epoxy resin. *Ind Eng Chem Res* 2015;54(32):7777-86.
- [35] Wen Y, Cheng Z, Li W, Li Z, Liao D, Hu X, et al. A novel oligomer containing DOPO and ferrocene groups: Synthesis, characterization, and its application in fire retardant epoxy resin. *Polym Degrad Stabil* 2018;156:111-24.
- [36] Levchik SV, Weil ED. Thermal decomposition, combustion and flame retardancy of epoxy resins—a review of the recent literature. *Polym Int* 2004;53(12):1901-29.
- [37] Wang X, Hu Y, Song L, Xing W, Lu H, Lv P, et al. Effect of a triazine ring-containing charring agent on fire retardancy and thermal degradation of intumescent flame retardant epoxy resins. *Polym Adv Technol* 2011;22(12):2480-7.
- [38] Zhang WC, He XD, Song TL, Jiao QJ, Yang RJ. The influence of the phosphorus-based flame retardant on the flame retardancy of the epoxy resins. *Polym Degrad Stabil* 2014;109:209-17.

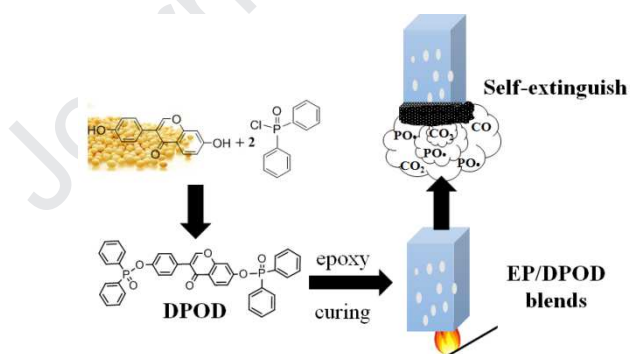
Synthesis of an organophosphorus flame retardant derived from daidzein and its application in epoxy resin

Chao Ma^{1,2}, Juan Li^{1,2}

1. Ningbo Key Laboratory of Polymer Materials, Ningbo Institute of Materials Technology and Engineering, Chinese Academy of Sciences, Ningbo, 315201, China.
2. Center of Materials Science and Optoelectronics Engineering, University of Chinese Academy of Sciences, Beijing, 100049, China.

Graphic abstract

DPOD, a flame retardant based on daidzein, plays an excellent flame retardant role in epoxy.



- ✧ A bio-based flame retardant PPA-C was prepared by using pyrophosphatic acid (PPA) and cytosine (C)
- ✧ UL-94 V0 rating is achieved for PP composites with 13.5 wt% PPA-C and 4.5 wt% PER.
- ✧ PPA-C/PER promotes the formation of intumescent char layer without defects.

Journal Pre-proof

CONFLICT OF INTEREST

We declare that we do not have any commercial or associative interest that represents a conflict of interest in connection with the work submitted.

Journal Pre-proof